

Supplement of Atmos. Meas. Tech., 12, 3453–3461, 2019
<https://doi.org/10.5194/amt-12-3453-2019-supplement>
© Author(s) 2019. This work is distributed under
the Creative Commons Attribution 4.0 License.



Supplement of

Measurements of delays of gas-phase compounds in a wide variety of tubing materials due to gas–wall interactions

Benjamin L. Deming et al.

Correspondence to: Paul J. Ziemann (paul.ziemann@colorado.edu) and Jose L. Jimenez (jose.jimenez@colorado.edu)

The copyright of individual parts of the supplement might differ from the CC BY 4.0 License.

Calculation of tubing delays

The depassivation time traces for the instrument only and combined instrument plus absorbent tubing
30 were fitted to exponential decays using Eq. (S1):

$$\frac{S}{S_0} = e^{-\frac{t}{\tau}} \quad (\text{S1})$$

where S is the measured signal at time t , S_0 is the signal before depassivation, and τ is the fitted
timescale. Calculating the time at which the measured signal decays to 90% of its final value is
equivalent to determining the point at which $\frac{S}{S_0}$ equals 0.1, which yields Eq. (S2):

$$35 \quad t = \tau \ln(10) \quad (\text{S2})$$

We then define the tubing delay for absorbent materials as the difference between the instrument only
delay and the instrument plus tubing delay, giving Eq. (S3):

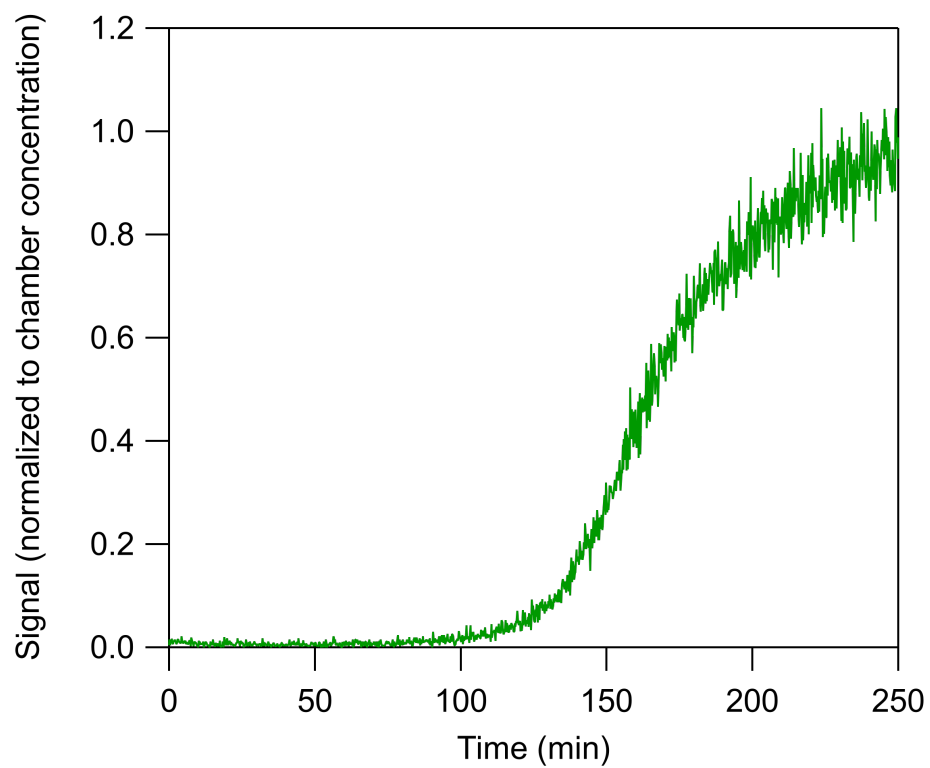
$$t_{tubing,abs} = \ln(10) (\tau_{total,abs} - \tau_{instrument}) \quad (\text{S3})$$

where $t_{tubing,abs}$ is the tubing delay for absorbent materials, $\tau_{instrument}$ is the instrument delay timescale,
40 and $\tau_{total,abs}$ is the timescale for depassivation of the instrument plus tubing.

The tubing delay for adsorbent materials is defined slightly differently. Namely, $t_{total,ads}$ is not
determined from an exponential fit (due to the sigmoidal shape of the time series), but by calculating the
point at which the signal reaches 50% of its maximum on passivation. An example time series is
presented in Fig. S1. The calculated value of $t_{total,ads}$ is corrected by the measured instrument delay to
45 give Eq. (S4):

$$t_{tubing,ads} = t_{total,ads} - \ln(10) \tau_{instrument} \quad (\text{S4})$$

where $t_{tubing,ads}$ is the adsorbent tubing delay time, $t_{total,ads}$ is the measured delay to 50% as described
above, and $\tau_{instrument}$ is the instrument delay timescale.



50

Figure S1. Time series of the delay of 20 ppbv of 2-decanone through approximately 0.6 m of aluminum tubing at RH = 0%. This is a typical tubing delay measurement for adsorbent tubing.

55

60

65 Sampling through Nafion tubing

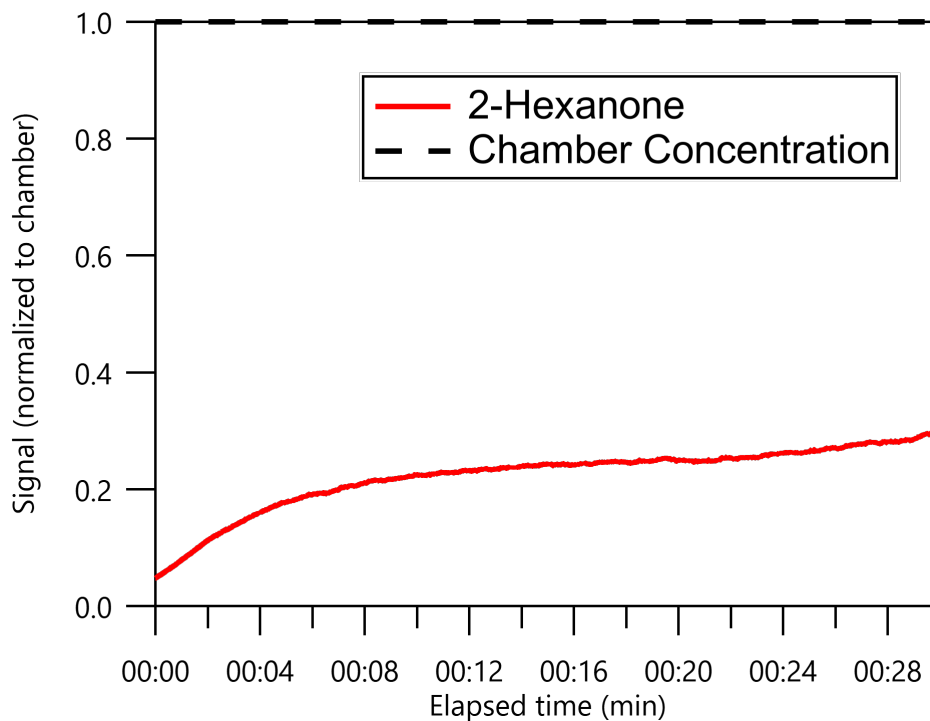


Figure S2. Time series of signal from 2-hexanone sampled through 0.6 m of Nafion tubing. No counter flow was passed over the Nafion, and signals from the other sampled 2-ketones were negligible over this time period.

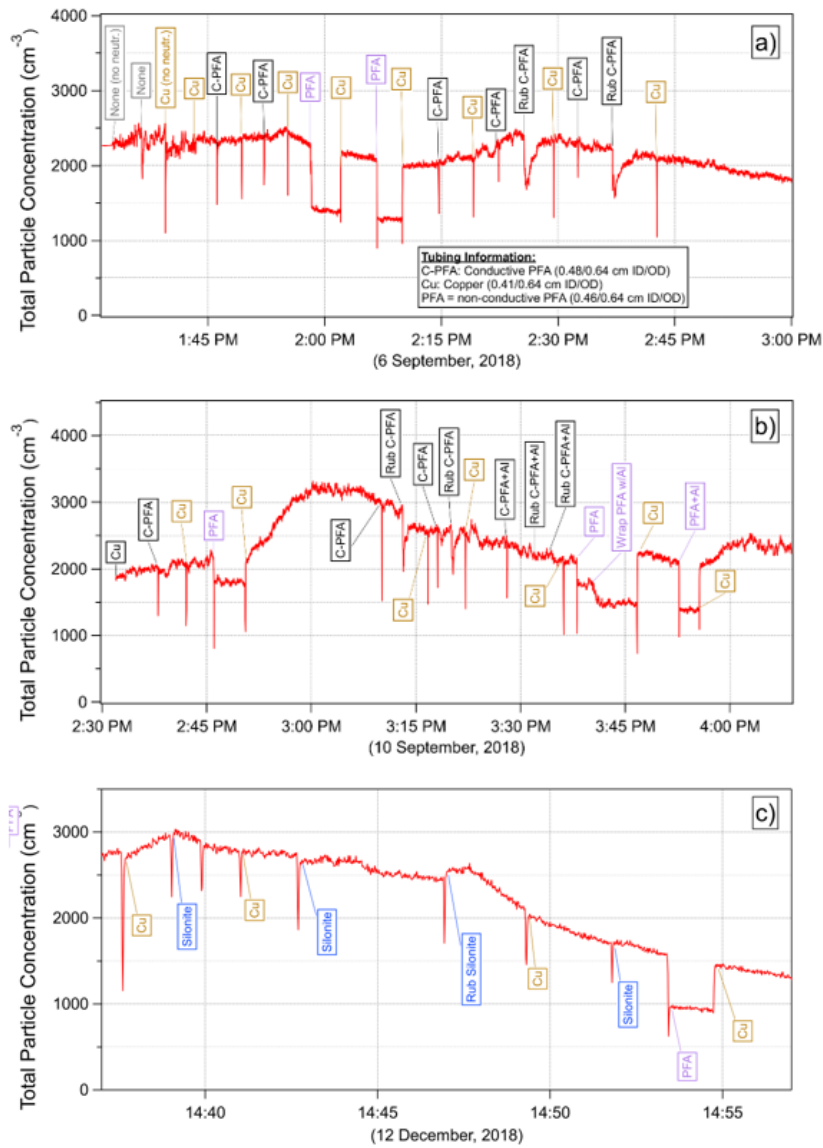
70

Losses of charged particles during transport through copper, PFA, and conductive PFA tubing

Fig. S3a shows no detectable particle losses in conductive PFA tubing compared to copper tubing. In contrast, non-conductive PFA tubing showed a consistent loss of ~35–40% of particles, possibly due to complete loss of particles of one charge polarity. Upon briefly (10s) rubbing the conductive PFA tubing with bare hands, however, an additional immediate loss of ~30% was observed followed by full recovery within ~1 min. During this measurement period the particle number distribution had a geometric mean \pm standard deviation of 76 ± 1.8 nm. Fig. S3b shows a similar response to rubbing the conductive PFA; however, after wrapping it in aluminum foil ("Al") no particle loss was observed upon rubbing as compared to sampling through copper tubing. One other observation is that when non-

75

80 conductive PFA tubing was retested it showed a smaller loss than the ~20% shown in Fig S3a, whereas
upon wrapping with aluminum foil the loss was more comparable to the ~35% seen before. This may be
because the non-conductive tubing had not been touched for several days, and handling it while
wrapping the foil caused it to build additional charge. During this measurement period the particle
number distribution had a geometric mean \pm standard deviation of 62 ± 2.0 nm. Fig S3c shows no losses
85 of particles through Silonite tubing, even after rubbing with bare hands. The particle number
distribution had a geometric mean \pm standard deviation of 70 ± 1.7 nm over this time.



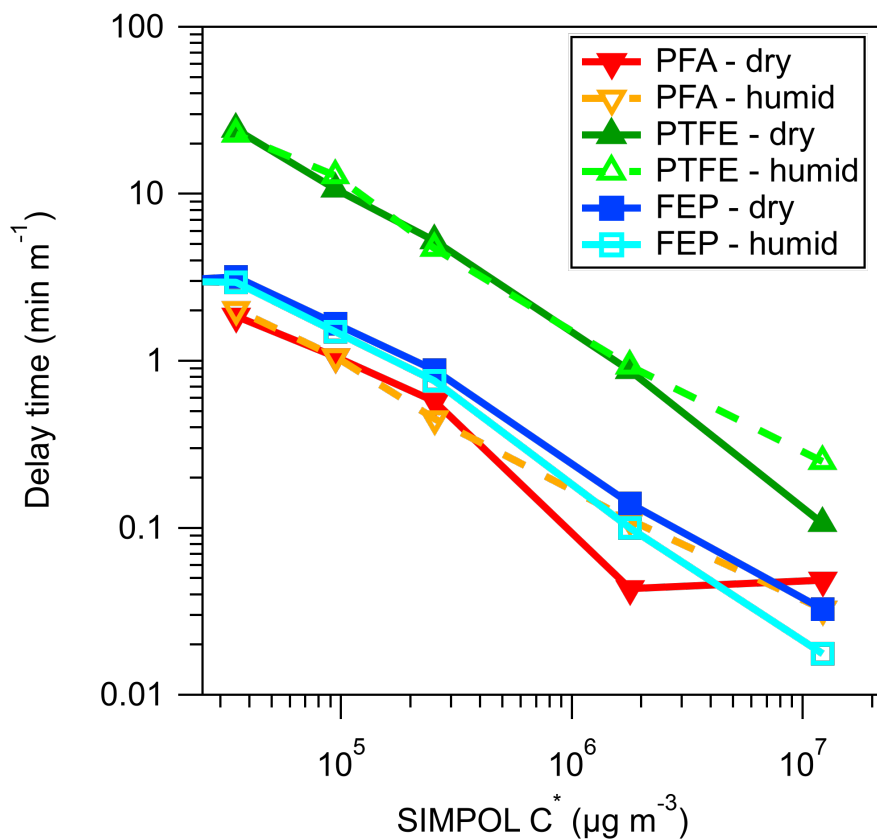
90

Figure S3. Time series of total particle number concentration (TSI CPC 3775, 1 LPM) while sampling laboratory (room) air. Measurements were alternated every few minutes by sampling through different tubing materials, while sampling through copper tubing between changes. All tubing was 1.5 meters long and nominally ¼” outer diameter (dimensions in legend). Tags indicating tubing material or activity are placed at the time when valves were switched or activity was initiated. All sampling was conducted through a TSI 3077 aerosol neutralizer unless otherwise indicated ("no neutr."). Sharp, brief (1-3 s) dips are from sampling particle-depleted air upon initial valve switching to tube that did not have flow for several minutes. Data shown are 1-s points. Residence time in the tubing was 8–11 s.

95

RH dependence of tubing delays for polymeric materials

A diagnostic used to label tubing materials as either absorbent or adsorbent was the humidity dependence of the measured tubing delay times. Tubing delays measured for a series of polymeric materials under both dry (<0.5% RH) and humid (45% RH) conditions are shown in Fig. S4. The similarity between the curves demonstrates a lack of humidity dependence and verifies that these delays are controlled by compound saturation vapor concentration C^* .



110 Figure S4. Comparison of tubing delay times measured under dry conditions (<0.5% RH, solid lines, darker colors) and humid conditions (45%RH, dashed lines, lighter colors).